Crossed and uncrossed visual pathways are impaired differently in open angle glaucoma patients

V. Parisi[1–3], G. L. Manni[1,2], D. Gregori[1], D. Olzi[1], S. Meconi[1],
G. Coppola[4], M. Scipioni[1], M. G. Bucci[1,2]

[1]Eye Clinic, 'Tor Vergata' University of Rome
[2]GB Bietti Foundation for Ophthalmology
[3]AfaR-RCCS, Eye Division, Fatebenefratelli Hospital, Rome
[4]II Neurological Clinic, 'La Sapienza' University of Rome

Introduction

Recent electrophysiological evaluations, performed by pattern electroretinogram (PERG) and visual evoked potential (VEP) recordings, suggest that patients affected by open angle glaucoma (OAG) present a retinal dysfunction and a delay in neural conduction in the postretinal visual pathways (Parisi 1997). Although an impairment of the innermost retinal layers (ganglion cells and their fibres) is well documented (Quigley et al. 1995), only recently has an impairment of the lateral geniculate nucleus (LGN) been observed in animals in which experimental glaucoma was induced (Weber et al. 2000). Therefore, it is supposed that the abnormal visual cortical responses observed in glaucoma may result from both retinal impairment and the involvement at the LGN level. In our previous study (Parisi 1997), the VEP responses were derived by means of a single electrode placed over both occipital cortexes and therefore did not allow a separate evaluation of the neural conduction along the crossed and uncrossed fibre visual pathways. On the basis of recent evidence regarding postretinal involvement in glaucoma, the aim of our work now is to evaluate the neural conduction in crossed and uncrossed visual pathways in OAG patients.

Patients and Methods

Twenty-two OAG patients (mean age 65.6 ± 9.5 years, refractive error between $+2$ and -2 sph) with mean deviation (MD) between -2 and -27 dB and corrected pattern standard deviation (CPSD) between $+2$ and $+13.5$ dB of 24/2 Humphrey computerized static perimetry, and with an IOP < 21 mmHg in at least one eye (average of the two highest values of the daily curve in medical treatment with β-blockers only), were enrolled. They were compared to 16 age-matched controls.

In OAP and control subjects, VEP recordings were performed as follows. The subjects under examination were seated in a semidark, soundproof room in front of a display with a uniform field of luminance of 5 cd/m^2 surround. Visual stimuli were full field checkerboard patterns (each square subtended an angle of 15′ of visual arc; contrast 80%, mean luminance 110 cd/m^2) generated on a TV monitor subtending 18°, and reversed in contrast at the rate of 2 reversal/ s. The refraction of all subjects was corrected for the viewing and no mydriatic or miotic drugs were used. Cup-shaped Ag/AgCl electrodes were fixed with collodion in positions: active electrode in O1 (left occipital cortex) and O2 (right occipital cortex (Jasper 1958), reference electrode in Fpz, with ground in the left arm. The inter-electrode resistance was kept <3 kΩ. The bioelectric signal was amplified (gain 20 000), filtered (bandpass 1–100 Hz) and averaged (200 events free from artifacts were averaged for each trial) by BM 6000. Analysis time was 200 ms. Stimulation was monocular after occlusion of the other eye and the bioelectrical cortical responses were recorded simultaneously in the homolateral visual (HC) cortex and in the contralateral visual cortex (CC), with respect to the stimulated eye. The transient VEP response is characterized by a number of waves with three subsequent peaks of negative, positive, negative polarity: N75, P100, N145.

We accepted VEP signals with signal-to-noise ratio >2. For all VEPs, the implicit time and the peak-to-peak amplitude of each of the averaged waves were measured directly on the displayed records by means of a pair of cursors The differences between-OAG patients and controls were evaluated by ANOVA, and linear regression analyses (Pearson's test) were used to establish the correlation between perimetric and VEP parameters.

Results

In OAG patients, the VEP P100 implicit times observed in HC and CC were both significantly ($P < 0.01$) delayed compared to those of the controls, and were significantly related ($P < 0.01$) to the MD observed in the nasal and the temporal hemi-fields, respectively (Table 1). We found an asymmetry in the bioelectrical responses obtained in HC and CC of all the OAG patients, and the intracortical differences (ID:P100 implicit time in HC–P100 implicit time in CC) converted to absolute values, were significantly higher than those of the controls (4.49 ± 3.72 ms and 1.16 ± 1.04 ms, respectively, $P = 0.001$). In 11 (50%) OAG patients, we observed an ID with a negative value (between -1 and -13.6 ms), indicating VEP P100 implicit times longer in CC than in HC, while in 11 (50%) OAG patients, we observed an ID with a positive value (between 1 and 8.8 ms), suggesting VEP
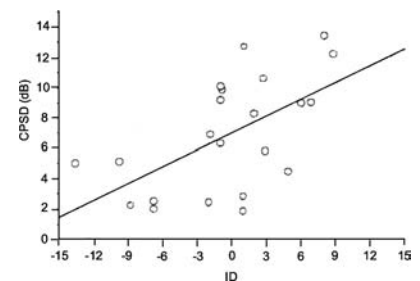

Fig. 1. Intracortical differences (ID:VEP P100 implicit times observed in homolateral cortex-VEP implicit times observed in Contralateral Cortex to the stimulated eye) of OAG patients plotted vs CPSD of Humphrey 24/2. Statistical analysis is reported in Table 1.

Table 1. Mean values and one ($\pm$) standard deviation of VEP P100 implicit time in OAG patients and controls.

	Control ($N = 16$) Mean $\pm$ SD (ms)	OAG ($N = 22$) Mean $\pm$ SD (ms)	OAG correlation between VEP P100 implicit time and Humphrey 24/2 parameters	
			MD	CPSD
Homolateral cortex	101.6 ± 2.2	$131.9 \pm 13.1^*$	$r = 0.570, P < 0.01$	$r = 0.170, P = 0.43$
Contralateral cortex	102.1 ± 2.6	$131.5 \pm 12.1^*$	$r = 0.703, P < 0.01$	$r = 0.570, P = 0.43$
Intracortical difference	1.16 ± 1.04	$4.49 \pm 3.72^*$	$r = 0.185, P = 0.583$	$r = 0.583, P = 0.004$

$^*P < 0.01$, ANOVA vs controls.

P100 implicit times longer in HC than in CC. The ID observed in OAG patients (ranging from -13.6 to $8.8\,\text{ms}$) was correlated significantly with the CPSD (r: 0.58, $P = 0.004$) (Fig. 1), but not with the MD (r: 0.18, $P = 0.409$).

Conclusions

The observed asymmetry in visual cortical responses suggests that crossed and un-crossed visual pathways could be impaired differently in OAG patients.

References

Jasper HH (1958): The ten-twenty electrode system of the International Federation of Electroencephalography. Clin Neurophysiol 10: 371–375.

Parisi V (1997): Neural conduction in the visual pathways in ocular hypertension and glau-coma. Graefes Arch Clin Exp Ophthalmol 235: 136–146.

Quigley HA, Nickells RW, Kerrigan LA et al. (1995): Retinal ganglion cell death in experimental glaucoma and after axotomy occurs by apoptosis. Invest Ophthalmol Vis Sci 36: 774–786.

Weber AJ, Chen H, Hubbard WC & Kaufman PL (2000): Experimental glaucoma and cell size, density and number in the primate lateral geniculate nucleus. Invest Ophthalmol Vis Sci 4: 1370–1379.

Reproducibility of a new technique to analyse retinal blood flow

M. Iester[1,2], M. Altier[1], P. Vittone[2], M. Zingirian[1], C. E. Traverso[1]

[1]Department of Neurological and Visual Sciences, Ophthalmology B, University of Genoa
[2]Division of Ophthalmology, G. Gaslini Institute, Genoa

Introduction

Indirect clinical data suggest that vascular factors could be glaucoma risk factors and therefore could be involved in the pathogenesis of the disease (Drance et al. 1988; Morgan & Drance 1975; Flammer 1994; Orgul & Flammer, 1994; Graham et al. 1995; Phelps & Corbett 1985; Hayreh et al. 1994). In this study, we tested the reproducibility of a non-invasive method able to evaluate the topograpy of perfused capillary vessels of the retina and optic nerve head with simultaneous evaluation of the blood flow variables.

Patients and Methods

Ten subjects were included in the study: 5 were classified as normal and 5 as having glaucoma. The diagnosis of primary angle glaucoma was based on the presence of typical glaucomatous visual field defect and optic disk damage. Normal subjects were recruited from those patients who had one eye with cataract and the other normal.

All the patients had their visual field analysed by Humphrey field analyser, program 30-2, full threshold SITA (Humphrey Inc., Leandro, CA, USA). Blood pressure and heart rate were assessed at the baseline.

Heidelberg retina flowmeter (HRF) combines the principles of a confocal scanning laser and a laser Doppler flowmeter (780 nm;

100 µW). Ater 128 scannings of each point of consideration, the HRF calculates a 2-dimensional map of the laser Doppler shift within a $300\,\mu\text{m}$ slice of tissue, over a rectangular area ($2.5° \times 10°$) of the posterior pole of the eye. The calculation is done using a fast-Fourier transformation. The laser Doppler shift values recorded at the different locations are displayed on the monitor in a colour code image. For each pixel, a frequency shift is calculated (Michelson & Schaumauss 1995; Michelson et al. 1996; Nicolela et al. 1997; Kagemann et al. 1998; Griesser et al. 1999).

The data were read by using a different programme called AFFPIA (automatic full field perfusion image analyser). The details of this technique are published elsewhere (Michelson et al. 1998). In brief, AFFPIA calculated the Doppler frequency shift and the haemodynamic factor or flow of each pixel according to the theory of Bonner and Nossal. For a valid estimation of retinal blood flow, some assumptions need to be made: brightness adequate, no artificial movement and Doppler shift below 2000 Hz. In order to meet these requirements, the resulting perfusion image was processed to account for underexposed and overexposed pixels, saccades and the retinal vessel tree. Using AFFPIA, the operator marked saccades and the location of the rim area. In a second step, the capillaries and large vessels of the retina were identifi-ed automatically by a vessel detection algorithm based on the intensity and the perfusion image. Then, underexposed and overexposed pixels and the saccades were automatically excluded. The local dishomo-geneities of the perfusion map were softened by a moving average procedure performed with a size of 5×5 pixels.

Based on this analysis, the blood flow was automatically analysed in the temporal, nasal and rim area. The heart beat-associated pulsation of capillary blood flow was evaluated by plotting the mean capillary flow of each horizontal line against time.

For each patient, three images were taken and analysed. When the intraimage-reproducibility was studied, the same observer (MI) analysed the flow maps 5 times and the COV was calculated. When the inter-image–intra-observer reproducibility was studied, the same observer (MI) analysed three different flow maps of the same patient once and the COV was calculated. All the images included either the superior ONH pole or the inferior ONH pole. When the images were analysed, temporal and nasal peripapillary retina and the optic rim area flow were calculated.

Results

The mean age was 68 ± 5.2 years (mean $\pm$ standard deviation) and the mean refractive error was -0.9 ± 1.9 dioptres. The visual field mean deviation was -3.1 ± 2.7 and corrected pattern standard deviation was -3.3 ± 1.6. Mean blood pressure and mean heart rate were 146.5/80 (systolic and diastolic blood pressure) and 80.7, respectively. When the intraimage–intra-observer reproducibility was studied the COV was 4.7%, ranging from 0.5% to 5% for the temporal area, 20.3% ranging from 0.5% to 28% for the rim area and 3.8% ranging from 0.1% to 5.3% for the nasal area. The analysed area